Stabilization of liquid active guests via nanoconfinement into a flexible microporous Metal-Organic Framework

Stabilization of liquid active guests *via* nanoconfinement into a flexible microporous metal–organic framework†

Author and affiliation details can be edited in the panel that appears to the right when you click on the author list.

Paolo P. Mazzeo,(0000-0002-5787-3609)[a,b], Davide Balestri,(0000-0003-3493-9115)[a], Alessia Bacchi,(0000-0001-5675-9372)[a,b,*] and Paolo Pelagatti,(0000-0002-6926-2928)[a,c,*]

[a]Dipartimento di Scienze Chimiche, della Vita e della Sostenibilità Ambientale, Università di Parma, Parco Area delle Scienze 17/A, 43124 Parma, Italy, alessia.bacchi@unipr.it, paolo.pelagatti@unipr.it

[b]Biopharmanet-TEC, Università di Parma, Parco Area delle Scienze 27/A, 43124 Parma, Italy

[c]Centro Interuniversitario di Reattività Chimica e Catalisi (CIRCC), Via Celso Ulpiani 27, 70126 Bari, Italy

Funding Information

We have combined the funding information you gave us on submission with the information in your acknowledgements. This will help ensure the funding information is as complete as possible and matches funders listed in the Crossref Funder Registry.

Please check that the funder names and award numbers are correct. For more information on acknowledging funders, visit our website: http://www.rsc.org/journals-books-databases/journal-authors-reviewers/author-responsibilities/#funding.

Funder Name :	Ministero dell'Istruzione, dell'Università e della Ricerca
Funder's main country of origin :	
Funder ID :	10.13039/501100003407
Award/grant Number :	Unassigned

Table of Contents Entry

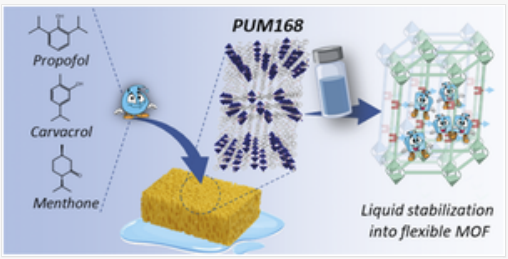

The nanoconfinement of the three liquid guests within a MOF has been fully investigated in terms of host–guest interactions and framework rearrangement.

Abstract

Liquid active ingredients are typically less stable than their solid analogues and they are also generally associated with storage and handling problems when considered for industrial usage. However, many synthetic and natural active ingredients are liquid or low melting solids under ambient conditions, and formulation or cocrystallization might be helpful to modulate this characteristic. As an alternative, crystalline porous matrices, such as metal–organic frameworks, can be used to encapsulate the guest molecules providing them with a crystalline environment very different to what might be observed in the pure liquid phase, thus stabilizing the active compounds in the solid state. In

this work, **PUM168**, a flexible heteroleptic MOF, has been used to encapsulate three liquid compounds (propofol, carvacrol and menthone). The nanoconfinement of the three guests has been fully investigated *via* SCXRD in terms of host–guest interactions and framework rearrangement as a function of the guest loading.

Introduction

When a pharmaceutical or agrochemical company evaluates a new compound, the solid formulation has significant advantages in terms of storage, handling and chemical stability. However, many synthetic and natural compounds are liquid or low melting solids under ambient conditions. In recent literature, cocrystallization appears as a strategic way to tune the physical properties of a molecule of interest, thus stabilizing the liquid component in the solid state.[1–11,63]

[Instruction: Please add here the following reference in the format that fit the style of the journal:
Bacchi Alessia, Mazzeo Paolo P. Cocrystallization as a tool to stabilize liquid active ingredients, Crystallography Review, 2021, DOI:10.1080/0889311X.2021.1978079.
Will all the reference numbers be then updated?
]The same concept has also been recently extended to toxic or explosive liquid compounds stabilized *via* cocrystallization.[8] An alternative type of crystalline framework that can be used to host liquid active compounds is represented by porous architectures. Molecular confinement in porous matrices is an emerging topic in supramolecular chemistry[12] aimed at tuning the properties of the guest which is in an environment substantially different from that corresponding to the bulk of the pure compound.[12–15] The structural and electronic properties of the guest can be drastically influenced by the geometrical constraints as well as the new supramolecular contacts imposed by the host.[16–20] Metal organic frameworks (MOFs) are among the most promising porous materials[21–30] being constituted by metal-containing nodes bridged by organic linkers.[29,31] Their success derives from their high functional and structural tunability, which has led MOFs to be superior materials in the storage,[32] separation[33] or transformation[34,35] of gases. MOFs have also been used for the encapsulation of drugs,[36,37] and organometallic catalysts[38–40] as well as food-related substances.[25,41] We herein want to use a porous MOF to encapsulate liquid guest molecules into a crystalline material. In this case, the driving force of the guest encapsulation into the MOF pores is related to the formation of the new host–guest intermolecular network,[19,42–45] and thus the fine interpretation of the guest location is fundamental to understanding the ultimate properties of the resulting material.[46] Molecular confinement in the microporous MOF **PUM168** (PUM = Parma University Material) has been recently investigated, providing a dynamic interpretation of the whole guest inclusion process (*i.e.* the concomitant substitution of a pristine solvent molecule as a consequence of the guest entrance) of phenol derivatives into a microporous MOF,[47] even in the case of multiple guest inclusion.[48] Although the investigation of the structural arrangement of the several guest molecules is a challenging task due to the partial occupancy of the guest molecules and their large thermal motion inside the MOF pores,[46,49,50] it has been recently shown that a careful structural analysis allows the determination of the molecular distribution of a rather large number of guest molecules within the pores of **PUM168**.[47,48] **PUM168** (Fig. 1) is a mixed-ligand MOF containing an amide functionalized bis-pyridine ligand, where the amide groups were considered to be the receptor sites for the uptake of hydrogen-bonded active guests. The adaptive behavior shown by **PUM168** allowed us to stepwisely ~~the~~ monitor~~ing of~~ the single-crystal-to-single-crystal transformations as a function of the guest loading, returning the detailed mechanism governing the solvent-to-guest exchange process occurring~~positioning~~ inside the channels and the concomitant~~ featuring the~~ framework rearrangement of **PUM168**~~ were observed.~~: eAmong the molecular guest at which **PUM168** have been already exposed, eugenol showed an almost exclusive preference for the carboxylate-containing paddle-wheel SBUs,[47] while thymol and carvacrol interacted preferentially with the amide groups.[48] This behaviour ~~which is~~ mirrors~~reflected in~~ the difference in the release properties of the guest from the loaded material. Moreover, eugenol was revealed to be the only guest able to completely remove DMF initially present in the pristine crystals.[47]

Fig. 1

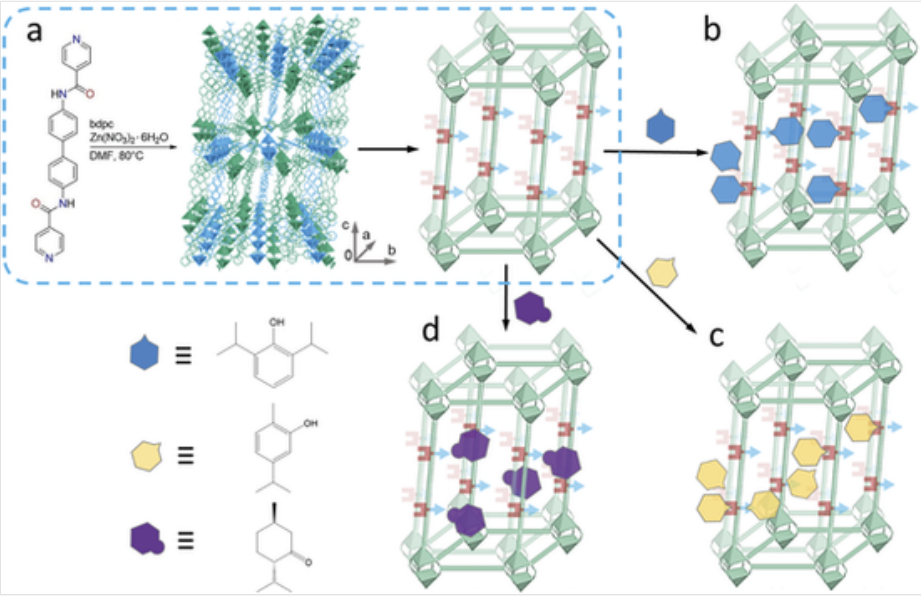

a. Synthesis of **PUM168** $[Zn_3(bpba)_{1.5}(bpdc)_3(DMF)_5]\cdot x$DMF and a perspective view of its triple interpenetrated structure along the crystallographic *a*-axis. Paddlewheel SBUs are represented as polyhedra while the organic ligands are shown in capped stick style: *c*-nets are shown in light blue while *a*-nets are shown in green. Schematic representation of the guests entering the **PUM168** pores in the case of soaking into b) propofol (mp: 18 °C), c) carvacrol (mp: 1 °C), and d) menthone (mp: −6 °C). Only the *a*-nets are reported for the sake of clarity. Amide groups are schematized to show the *cis*-configuration: the red blocks represent the C═O moieties while the blue arrows represent the N–H moieties.

To extend the study to a larger number of guests and to make a step forward towards the understanding of the variables governing the efficacy of the guest loading, here we report on the nanoconfinement of three pure liquid active molecules, propofol, carvacrol and menthone (Fig. 1b–d), into **PUM168**. Propofol (2,6-diisopropylphenol) is commonly used for the induction and maintenance of general anaesthesia and sedation and appears on the WHO Model List of Essential Medicines.[51] It has extremely low aqueous solubility that justifies its use as injectable emulsion. Carvacrol (2-methyl-5-isopropyl phenol) and menthone (2-isopropyl-5-methyl-cyclohexanone) are essential oil components with known antibacterial and antimycotic properties and are extracted from oregano and mint, respectively.[52–54]

Although the loading capacity of **PUM168** towards carvacrol is partly known,[48] its inclusion as pure liquid has never been reported. Propofol has two isopropyl moieties close to the hydroxyl groups, allowing the evaluation of the steric encumbrance on the loading capacity. Finally, menthone has a structure significantly different from that of the guests investigated so far. It is not aromatic and does not contain an O–H group, although it has the same alkyl substituents as those of carvacrol.

Hence, in this article we focus our efforts on the structural analysis of the role the anchoring sites characterizing the inner walls of the MOF, in synergy with the overall framework flexibility, play toward the final stabilization of the liquid components into the crystalline framework of the *ad hoc* synthesized **PUM168**.

Results and discussion

PUM168 ~~(ref. 47)~~[Instruction: please add the reference in the standard ref format.] is an adaptive heteroleptic MOF whose flexible framework is constituted by 2D square layers formed by Zn-paddlewheel-SBUs linked by rigid linear di-carboxylate anions (4,4′-biphenylene-dicarboxylate, bpdc), pillared by *N*,*N*′-(1,1′-biphenyl)-4,4′-diylbis-4-pyridinecarboxamide ligands (bpba).[55] Its formula is $[Zn_3(bpba)_{1.5}(bpdc)_3(DMF)_5]\cdot x$DMF. The inner pores are decorated with the amide groups of the bpba ligands, which represent good H-bond anchoring sites for the guest molecules. The pores of the native **PUM168** are occupied by pristine DMF molecules coming from the solvothermal synthesis (DMF, *N*,*N*′-dimethylformamide). A fraction of the DMF molecules are hydrogen-bonded to the MOF amide groups (Fig. S1†). **PUM168** is triply interpenetrated with two symmetry related acentric nets (*a*-nets) and one centric net (*c*-net). Despite the interpenetration, the structure presents microporous meandering channels which represent 49.7% of the total cell volume. As reported in detail in the Experimental section, the native crystals of **PUM168** were directly soaked into pure liquid compounds without prior MOF activation (*i.e.* the native solvent

removal). In all cases, the soaking was prolonged for seven days at room temperature, a period sufficient to reach equilibration, as previously determined.[46,47] SCXRD results have been extensively discussed across the paper emphasizing the role of the adaptive framework as a function of the loading guest. Crystallographic structural information is reported in Tables 1 and SI1.†

Table 1

Crystallographic data for **PUM168**@propofol, **PUM168**@carvacrol, **PUM168**@menthone

Identification code	PUM168@propofol	PUM168@carvacrol	PUM168@menthone
Empirical formula	$C_{126.62}H_{125.75}N_{7.62}O_{20.25}Zn_3$	$C_{130.35}H_{132.3}N_{8.95}O_{22.3}Zn_3$	$C_{94}H_{83}N_8O_{18}Zn_3$
Formula weight	2274.45	2377.15	1805.03
Temperature/K	100	100	100
Crystal system	Triclinic	Triclinic	Triclinic
Space group	$P\bar{1}$	$P\bar{1}$	$P\bar{1}$
Z	4	4	2
a/Å	15.263(3)	21.473(5)	15.186(3)
b/Å	30.497(6)	21.5530(9)	15.210(3)
c/Å	26.950(5)	26.886(2)	26.964(5)
α/°	89.20(3)	94.896(3)	91.53(3)
β/°	82.16(3)	102.406(8)	102.04(3)
γ/°	87.80(3)	89.986(14)	91.69(3)
Volume/Å^3	12 417(4)	12 106(3)	6085(2)
Radiation	$\lambda = 0.700$ Å	$\lambda = 0.700$ Å	$\lambda = 0.700$ Å
Independent reflections	46 776	59 226	22 884
	$R_{int} = 0.0316$	$R_{int} = 0.0281$	$R_{int} = 0.0268$
	$R_{sigma} = 0.0227$	$R_{sigma} = 0.0219$	$R_{sigma} = 0.0177$
Final R indices [$I \geqq 2\sigma(I)$]	$R_1 = 0.0898$	$R_1 = 0.0534$	$R_1 = 0.0713$
	$wR_2 = 0.2695$	$wR_2 = 0.1407$	$wR_2 = 0.2002$
Final R indices [all data]	$R_1 = 0.0918$	$R_1 = 0.0589$	$R_1 = 0.0713$
	$wR_2 = 0.2716$	$wR_2 = 0.1462$	$wR_2 = 0.2007$
Largest diff. peak/hole/e Å^{-3}	2.34/−1.43	1.28/−1.16	1.04/−0.87

Host–guest interactions

Propofol and carvacrol are both phenol derivatives with a hydroxyl group that can act as a hydrogen bond donor as well as a hydrogen bond acceptor. This group makes the selected guests ideal candidates to establish intermolecular interactions with the inner walls of the **PUM168** pores. In **PUM168**@propofol, the guest molecules mainly interact with both the non-equivalent bpba ligands of the *a*-net. Hence, propofol-B and propofol-F (see Fig. 2a) are linked to the bpba ligand through the C═O of the amidic moieties (O⋯O = 2.845(3) Å and 2.927(8) Å, respectively), while propofol-C and propofol-G bind to the amidic moieties through the N–H functionalities (N⋯O = 3.061(3) Å and 3.021(7) Å, respectively). Propofol-D also binds to the *a*-net through the N–H functionality of the amide group (N⋯O = 3.230(3) Å). Three different propofol dimers have also been observed: propofol-H and propofol-I form a dimer linked to the *a*-net (O⋯O = 2.62(2) Å), and DMF-III is then bridged to propofol-I (Fig. 2a). Two additional partially

occupied face-to-face dimers (propofol-A/A′ O···O = 2.940(2) Å and propofol-E/E′ O···O = 2.727(2) Å) loosely bound to the **PUM168** walls have also been modelled. It is worth recalling that pure propofol crystallizes as a H-bonded tetramer (CCDC code GAPTOG[56]), with a square arrangement of four hydroxyl groups with an average O···O distance of 2.73 Å, which is similar to that observed for the nanoconfined guest molecules into **PUM168**. The number of the structurally modelled molecules of propofol is 3.5 per asymmetric unit of **PUM168**, corresponding to 7.8% weight loading. These data are very similar to that found with eugenol, for which 4 molecules of the guest were found.[46] Taking into account the potential void volume in **PUM168**@propofol and the molecular volume of the guest, a ~~loading process efficient parameter~~loading efficiency parameter of 30% was calculated (see the ESI †). In **PUM168**@carvacrol, the pristine solvent is still linked to the framework through the amidic groups: DMF-I and DMF-II are still H-bonded to the *c*-net, while DMF-III and DMF-V are H-bonded to the *a*-net. Similar to propofol, carvacrol acts both as a H-bond donor and acceptor and then the formation of homodimers is again observed. Carvacrol-A/B homodimer bridges the *a*-net and *c*-net (Fig. 2b); in particular, carvacrol-A acts as a H-bond donor to the C=O of the amide group of the *c*-net (O···O distance of 2.784(3) Å) and as a H-bond acceptor with respect to the carvacrol-B (O···O distance of 2.876(4) Å). The latter, in turn, exploits its H-bond acceptor character with the N–H of the amide group of the adjacent *a*-net (N···O distance of 3.063(3) Å). Carvacrol-C acts as a H-bond donor and binds to the *a*-net through the C=O of the amide group (O···O distance of 2.733(5) Å) and, as a H-bond acceptor, it bridges carvacrol-D (O···O distance of 2.825(2) Å). The homodimer carvacrol-C/D is very disordered and different mutually exclusive positions have been modelled. For the sake of clarity, as shown in Fig. 2b, only one of the disordered positions is shown in orange and ellipsoid style. Carvacrol-F/G binds to the non-equivalent acentric bpba ligand thus forming another homodimer. Carvacrol-F is linked to the N–H of the bpba ligand (N···O distance of 3.063(3) Å), bridging carvacrol-G (O···O distance of 2.760(4) Å), which in turn binds to an extra DMF molecule (DMF-IV, O···O distance of 2.695(5) Å). Carvacrol-E and carvacrol-H, acting as H-bond donors, bind reciprocally to the non-symmetric related bpba ligand of the *a*-net (O···O distance of 2.806(6) Å and 2.690(3) Å). An extra guest molecule, carvacrol-I, shares the binding site with DMF-V and then bridges an extra solvent molecule, DMF-VI. A summary of the host–guest interactions and guest occupancy is reported in the ESI.† The number of structurally modelled molecules of carvacrol is 3.5 per asymmetric unit of **PUM168**, corresponding to 6.3% weight loading, a value similar to that found with propofol. Also, the calculated loading efficiency parameter, 32%, was very close to that found with propofol, in accordance with the similarity of the guest molecular volumes (see the ESI†). Differently from the phenol derivatives, menthone contains a carbonyl group that can only act as a H-bond acceptor (Fig. 1) towards the N–H amide groups but its structural determination within the **PUM168** pores is way more complicated than the above-mentioned guests. Only one single molecule of menthone is, in fact, clearly observed, namely menthone-A, while two pristine DMF molecules have been identified binding to the *c*-net (DMF-I) and the *a*-net (DMF-II) (Fig. 3). The non-aromatic behavior of the guest might influence its mobility through the MOF channels thus preventing effective binding to the pore walls. The overall disorder affecting both the guest molecules and the framework makes the structural identification very demanding and an extensive electron density remained undefined (see the ESI†).

Fig. 2

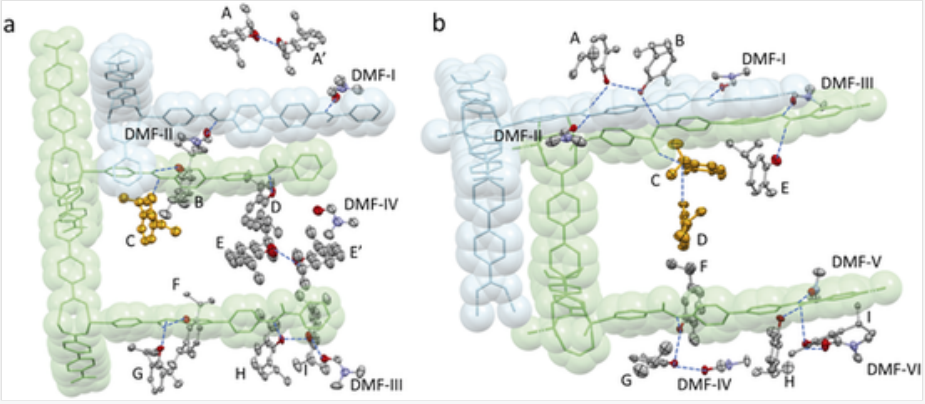

Host–guest and guest–guest interactions in a. **PUM168**@propofol and b. **PUM168**@carvacrol. *c*-Nets are shown in light blue while *a*-nets are shown in green. H-Bonds are highlighted by dashed blue lines. Guests are shown as ellipsoids at 50% probability level. Hydrogen atoms are omitted for the sake of clarity. Propofol-C and carvacrol-C, D are largely affected by positional disorder and thus

only one position is reported and shown in orange for the sake of clarity. Resilient DMF molecules are also displayed. Conformational disorder of the nets is removed for the sake of clarity.

Fig. 3

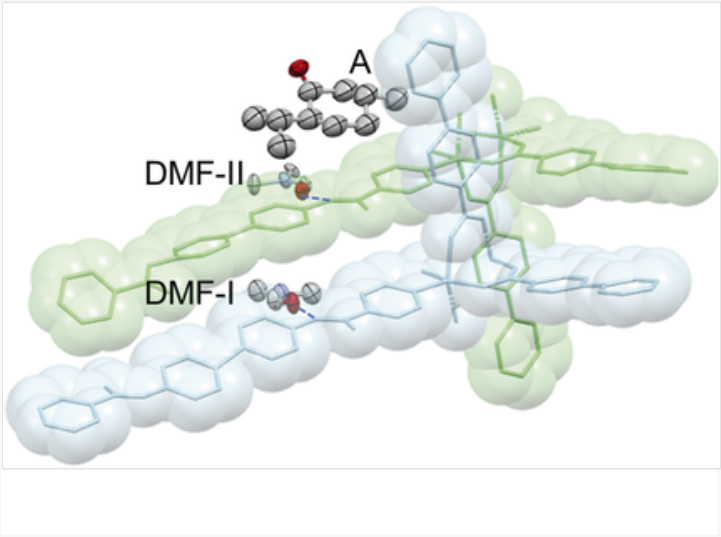

Host–guest and guest–guest interactions in **PUM168**@menthon. *c*-Nets are shown in light blue while *a*-nets are reported in green. Guests are shown as ellipsoids at 50% probability level. H-Bonds are highlighted by dashed blue lines. Hydrogen atoms are omitted for the sake of clarity. Resilient DMF molecules are also displayed. Conformational disorder of the nets is removed for the sake of clarity.

MOF flexibility

The inclusion of the different guests into the MOF pores leads to different structural rearrangements of the crystalline host framework. As shown in Fig. 4, a comparison between the nets as observed in the pristine structure (Fig. 4a) and those observed as a function of the guest loading (Fig. 4b–d) is reported. The adaptive behaviour of the framework towards the entering guest is evident by looking at the different organization adopted by the same nets in all the **PUM168**@guest crystals.

Fig. 4

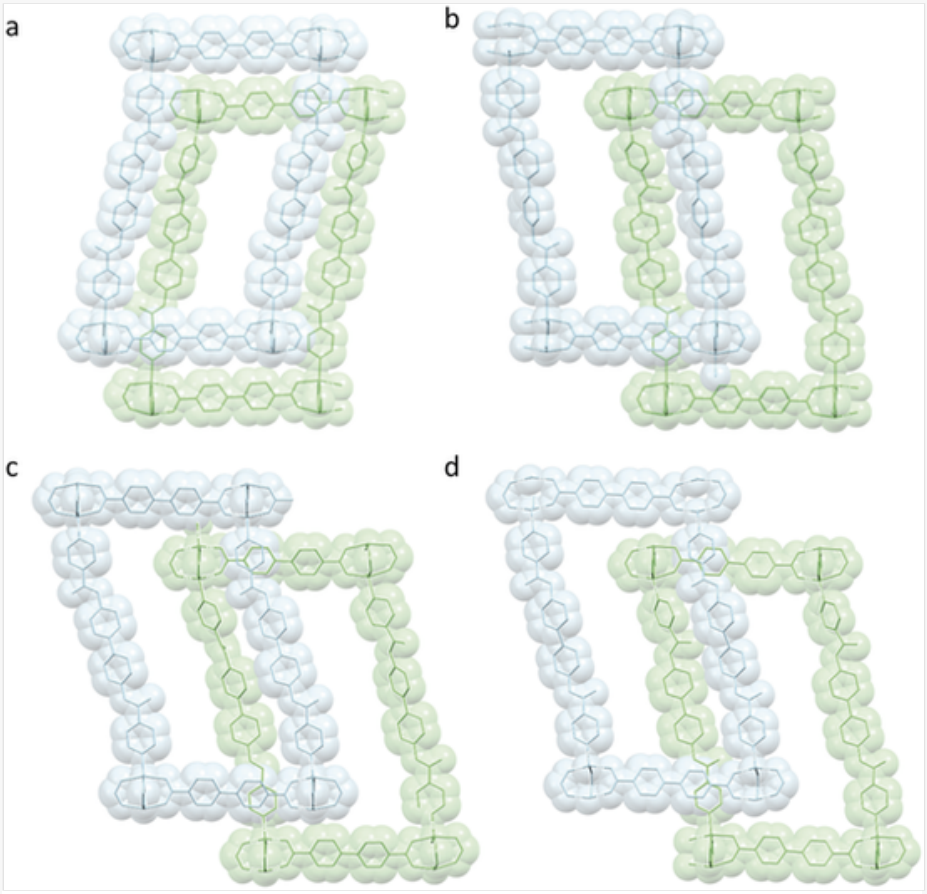

Comparison between the a) pristine **PUM168** framework[47,48] and after soaking in b) propofol, c) carvacrol and d) menthone. *c*-Nets and *a*-nets are shown in light blue and green, respectively. Hydrogen atoms are omitted for the sake of clarity.

The high flexibility and robustness of the framework are mainly due to the presence of the pillar linkers that, thanks to their flexible amidic moieties, can dynamically accommodate a progressive number of incoming guest molecules. The conformational rearrangement typically involves the *a*-net with the replacement of the anchored pristine DMF molecules by the entering guests. The *c*-net, instead, is not involved in the formation of host–guest interactions and the native solvent molecules remain H-bonded to the amidic moieties. The inclusion of propofol is associated with an extended conformational disorder of the amidic linker, indicating the partial *cis*-to-*trans* conformational isomerization of the amide groups which both interact with the propofol guest molecule, which is thus modelled in two concomitant and mutually exclusive positions alternately exploiting its H-bond donor and acceptor character (Fig. S3 †). The inclusion of carvacrol also led the bpba linker to rearrange: the torsion angle between the amide groups of the bpba ligands of the *a*-net moves from the cis configuration to ~90°. The conformational disorder of the amide linkers in both

cases is also related to the variation of the cell parameters. The crystallographic *c*-axis coincides with the pillar length, which thus remains almost constant in all the **PUM168**@guest materials, with values ranging between 26.89 Å and 26.96 Å. The carboxylate square grids lay, instead, on the {001} crystallographic planes and thus the *a*- and *b*-axis values are more influenced by the overall network rearrangement as a function of the guest loading (see Table 1). In **PUM168**@carvacrol, the loss of translational order due to the staggered conformation of the nets results in a difference both in the cell orientation and dimensions while in **PUM168**@propofol, the conformational change of the bpba linkers lead to the doubling of the *b*-axis (see Table 1 and Fig. 5).

Fig. 5

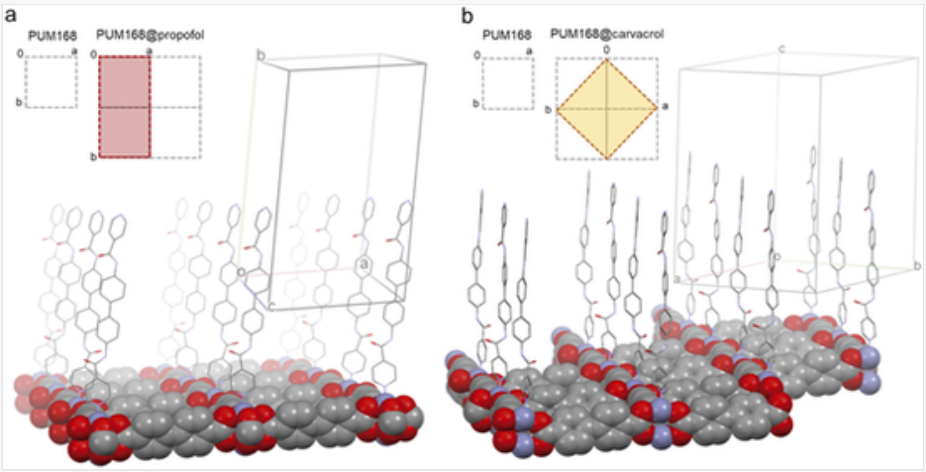

Details of the conformational arrangement of the *a*-net in a. **PUM168**@propofol and b. **PUM168**@carvacrol. The carboxylate grids perpendicular to the *c*-axis are shown in spacefill style while the bpba linkers are shown in wireframe style. The disorder of the bpba linkers is omitted for the sake of clarity. Insets: Details of the cell axis variation as a function of the guest loading.

Experimental

Materials and methods

N,*N*′-(Biphenyl-4,4′-diyl)-di-isonicotinamide (bpba) was prepared according to a previously described method slightly modified.[55] All other reagents and solvents were used as received, including 4,4′-biphenyldicarboxylic acid, zinc nitrate hexahydrate and *N*,*N*-dimethylformamide. **PUM168** has been synthesized *via* a solvothermal route in DMF solvent at 80 °C obtaining large single crystals. The details are reported in the ESI.[†]

X-ray single crystal data collections (SCXRD) of all samples were performed at Elettra Sincrotrone (Trieste, Italy), beamline XRD1.[57] MOF crystals were soaked in pure liquid guest for one week at room temperature, and then picked up and mounted with cryoloops (0.05–0.3 mm). The beamline spectra (produced by a NdBFe multipole wiggler) were monochromatized to 17.71 keV (0.700 Å) through a Si(111) double crystal monochromator and focused to obtain a beam size of 0.2 × 0.2 mm FWHM at the sample (photon flux: 10^{12}–10^{13} ph s^{-1}). Datasets were collected at 100 K (nitrogen stream was supplied through an Oxford Cryostream 700) through a rotating crystal method. For the triclinic crystals, complete datasets were obtained by merging two different data collections performed on the same crystal, mounted with different orientations. Measurements were performed using a monochromatic wavelength of 0.700 Å on a Pilatus 2M hybrid-pixel area detector. The diffraction data were indexed and integrated using XDS.[58]

Scaling was done using CCP4-Aimless.[59] For single phi scan acquisition, data were indexed, integrated, and scaled using CrysAlisPRO v.1.171.38.41 software (Rigaku Oxford Diffraction).

The structures were solved by the intrinsic phase algorithm implemented in SHELXT[60] in Olex2 v1.3.[61] Fourier analysis and refinement were performed by the full-matrix least-squares methods based on F^2 implemented in SHELXL.[62] For all the structures, anisotropic displacement parameters were refined except for hydrogen atoms. For all structures, anisotropic displacement parameters were refined except for hydrogen atoms. Crystal data for the compounds isolated in this work are reported in Tables 1 and SI.[†] ORTEP diagrams of all the compounds characterized

here are reported in the ESI.[†] Crystallographic data for the structures **PUM168**@propofol, **PUM168**@carvacrol and **PUM168**@menthone have been deposited in the CSD with the CCDC 2094688–2094690 refcodes.

Conclusions

The stabilization of active liquid compounds in a solid matrix is a topic of interest in all the areas where solid formulations are used. An alternative to the widely applied cocrystallization with suitable coformers is represented by the encapsulation of the active ingredient into porous host matrices. *Ad hoc* engineered metal organic frameworks can provide the right crystalline environment for the entrance and stabilization of the liquid ingredient into their pores. When the host–guest interactions are sufficiently robust, a detailed mapping of the guest distribution inside the MOF pores becomes feasible, as well as a model of the structural rearrangements undergone by the host, leading to the deciphering of the loading mechanism. In this article, we have shown that the microporous MOF **PUM168** is capable of exchanging the pristine DMF molecules with a rather large number of molecules of two liquid phenol derivatives, such as propofol and carvacrol. The process occurs through single-crystal-to-single-crystal transformations under ambient conditions. An in-depth structural analysis of the loaded crystals has highlighted the structural organization adopted by the two guests inside the MOF pores, where the most stabilizing host–guest interactions are represented by hydrogen bond contacts involving the OH groups of the guests with the amide groups installed in the inner walls of the MOF pores. Contrary to what was observed with eugenol, in these cases, it has not been possible to remove completely the pristine DMF, probably because of the steric encumbrance generated by the branched alkyl substituents featuring the two phenol derivatives, which hampers the travelling of the guest molecules inside the crystal. The guest molecules used, drive the formaton of the host-guest intermolecular network, which, in turn, influences the distortion of the MOF.~~imposed intermolecular contacts involving the amide groups provokes their conformational rearrangement that, in turn, results in guest-dependent distortions of the MOF framework.~~ This adaptive behaviour of the host scaffold is at the basis~~e~~ of the guest inclusion capacity of **PUM168**. Indeed, the loading of a guest devoid of an OH group, such as menthone, resulted in a modest loading featured by poor host–guest interactions that do not provoke a significant distortion of the initial host framework. In conclusion, the importance of the ability of the host framework to rearrange during guest loading has been demonstrated, as excellently detailed by Nassimbeni[19,43,49] with pure organic hosts.

Conflicts of interest

There are no conflicts to declare.

Acknowledgements

The authors would like to thank Dr. Nicola Demitri (Elettra Synchrotron Trieste) for technical assistance. This work has benefited from the equipment and framework of the COMP-HUB Initiative, funded by the "Departments of Excellence" program of the Italian Ministry for Education, University and Research (MIUR, 2018–2022). COST Action CA18112—Mechanochemistry for Sustainable Industry is acknowledged.

References

1 P. P. Mazzeo, C. Carraro, A. Monica, D. Capucci, P. Pelagatti, F. Bianchi, S. Agazzi, M. Careri, A. Raio, M. Carta, F. Menicucci, M. Belli, M. Michelozzi and A. Bacchi, *ACS Sustainable Chem. Eng.*, 2019, **7**, 17929–17940.

2 P. P. Mazzeo, S. Canossa, C. Carraro, P. Pelagatti and A. Bacchi, *CrystEngComm*, 2020, **22**, 7341–7349.

3 P. P. Mazzeo, C. Carraro, A. Arns, P. Pelagatti and A. Bacchi, *Cryst. Growth Des.*, 2020, **20**, 636–644.

4 D. Capucci, D. Balestri, P. P. Mazzeo, P. Pelagatti, K. Rubini and A. Bacchi, *Cryst. Growth Des.*, 2017, **17**, 4958–4964.

5 S. C. McKellar, A. R. Kennedy, N. C. McCloy, E. McBride and A. J. Florence, *Cryst. Growth Des.*, 2014, **14**, 2422–2430.

6 A. Bacchi, D. Capucci, M. Giannetto, M. Mattarozzi, P. Pelagatti, N. Rodriguez-Hornedo, K. Rubini and A. Sala, *Cryst. Growth Des.*, 2016, **16**, 6547–6555.

7 C. B. Aakeröy and D. J. Salmon, *CrystEngComm*, 2005, **7**, 439–448.

8 C. Aakeröy, W. Tharanga, J. Benton and J. Desper, *Chem. Commun.*, 2015, **51**, 2425–2428.

9 C. Aakeroy, *Acta Crystallogr., Sect. B: Struct. Sci., Cryst. Eng. Mater.*, 2015, **71**, 387–391.

10 F. Bianchi, F. Fornari, N. Riboni, C. Spadini, C. S. Cabassi, M. Iannarelli, C. Carraro, P. P. Mazzeo, A. Bacchi, S. Orlandini, S. Furlanetto and M. Careri, *Food Chem.*, 2021, **347**, 129051.

11 D. Braga, F. Grepioni, L. Maini, P. P. Mazzeo and K. Rubini, *Thermochim. Acta*, 2010, **507**–**508**, 1–8.

12 G. Tabacchi, *ChemPhysChem*, 2018, **19**, 1249–1297.

13 J. Y. Chung, C. W. Liao, Y. W. Chang, B. K. Chang, H. Wang, J. Li and C. Y. Wang, *J. Phys. Chem. C*, 2017, **121**, 27369–27378.

14 B. E. Souza, S. Rudić, K. Titov, A. S. Babal, J. D. Taylor and J. C. Tan, *Chem. Commun.*, 2019, **55**, 3868–3871.

15 G. Srinivas, W. Travis, J. Ford, H. Wu, Z. X. Guo and T. Yildirim, *J. Mater. Chem. A*, 2013, **1**, 4167–4172.

16 M. H. Köhler, J. R. Bordin, C. F. de Matos and M. C. Barbosa, *Chem. Eng. Sci.*, 2019, **203**, 54–67.

17 I. Bassanetti, S. Bracco, A. Comotti, M. Negroni, C. Bezuidenhout, S. Canossa, P. P. Mazzeo, L. Marchió and P. Sozzani, *J. Mater. Chem. A*, 2018, **6**, 14231–14239.

18 P. P. Mazzeo, L. Maini, D. Braga, G. Valenti, F. Paolucci, M. Marcaccio, A. Barbieri and B. Ventura, *Eur. J. Inorg. Chem.*, 2013, 4459–4465.

19 L. R. Nassimbeni, *Acc. Chem. Res.*, 2003, **36**, 631–637.

20 Y. Inokuma, S. Yoshioka, J. Ariyoshi, T. Arai, Y. Hitora, K. Takada, S. Matsunaga, K. Rissanen and M. Fujita, *Nature*, 2013, **495**, 461–466.

21 F. Bianchi, A. Pankajakshan, F. Fornari, S. Mandal, P. Pelagatti, A. Bacchi, P. P. Mazzeo and M. Careri, *Microchem. J.*, 2020, **154**, 1–7.

22 J. Guo, B. D. Mattos, B. L. Tardy, V. M. Moody, G. Xiao, H. Ejima, J. Cui, K. Liang and J. J. Richardson, *Curr. Med. Chem.*, 2018, **26**, 6107–6131.

23 D. Balestri, P. Scilabra, C. Carraro, A. Delledonne, A. Bacchi, P. P. Mazzeo, L. Carlucci and P. Pelagatti, *CrystEngComm*, 2019, **21**, 6365–6373.

24 D. Braga, L. Maini, P. P. Mazzeo and B. Ventura, *Chem. – Eur. J.*, 2010, **16**, 1553–1559.

25 P. L. Wang, L. H. Xie, E. A. Joseph, J. R. Li, X. O. Su and H. C. Zhou, *Chem. Rev.*, 2019, **119**, 10638–10690.

26 K. K. Tanabe and S. M. Cohen, *Chem. Soc. Rev.*, 2011, **40**, 498–519.

27 A. Schneemann, V. Bon, I. Schwedler, I. Senkovska, S. Kaskel and R. A. Fischer, *Chem. Soc. Rev.*, 2014, **43**, 6062–6096.

28 C. S. Diercks, M. J. Kalmutzki, N. J. Diercks and O. M. Yaghi, *ACS Cent. Sci.*, 2019, **6**, 57.

29 A. Schoedel and O. M. Yaghi, Porosity in Metal–Organic Compounds, 2016

30 M. Eddaoudi, J. Kim, N. Rosi, D. Vodak, J. Wachter, M. O'Keeffe and O. M. Yaghi, *Science*, 2002, **295**, 469–472.

31 H. C. J. Zhou and S. Kitagawa, *Chem. Soc. Rev.*, 2014, **43**, 5415–5418.

32 T. Qiu, Z. Liang, W. Guo, H. Tabassum, S. Gao and R. Zou, *ACS Energy Lett.*, 2020, **5**, 520–532.

33 H. Wang and J. Li, *Acc. Chem. Res.*, 2019, **52**, 1968–1978.

34 H. Zhang, J. Li, Q. Tan, L. Lu, Z. Wang and G. Wu, *Chem. – Eur. J.*, 2018, **24**, 18137–18157.

35 J. Liang, Y. B. Huang and R. Cao, *Coord. Chem. Rev.*, 2019, **378**, 32–65.

36 J. Yang and Y. W. Yang, *Small*, 2020, **16**, 1–24.

37 Y. Wang, J. Yan, N. Wen, H. Xiong, S. Cai, Q. He, Y. Hu, D. Peng, Z. Liu and Y. Liu, *Biomaterials*, 2020, **230**, 119619.

38 C. T. Buru and O. K. Farha, *ACS Appl. Mater. Interfaces*, 2020, **12**, 5345–5360.

39 D. Balestri, Y. Roux, M. Mattarozzi, C. Mucchino, L. Heux, D. Brazzolotto, V. Artero, C. Duboc, P. Pelagatti, L. Marchiò and M. Gennari, *Inorg. Chem.*, 2017, **56**, 14801–14808.

40 L. J. Jongkind, X. Caumes, A. P. T. Hartendorp and J. N. H. Reek, *Acc. Chem. Res.*, 2018, **51**, 2115–2128.

41 N. Manousi, G. A. Zachariadis, E. A. Deliyanni and V. F. Samanidou, *Molecules*, 2018, **23**, 1–21.

42 E. J. Tiffin, N. M. Sykes, E. Weber, N. Ravenscroft and L. R. Nassimbeni, *Cryst. Growth Des.*, 2019, **19**, 1880–1887.

43 F. M. Amombo Noa, S. A. Bourne, H. Su and L. R. Nassimbeni, *Cryst. Growth Des.*, 2017, **17**, 4647–4654.

44 P. P. Mazzeo, A. Bacchi and P. Pelagatti, *Coord. Chem. Rev.*, 2020, **414**, 1–17.

45 M. Pioli, C. Loffi, P. P. Mazzeo, A. Bacchi and P. Pelagatti, *Inorg. Chim. Acta*, 2020, **517**, 120190.

46 K. Rissanen, *Chem. Soc. Rev.*, 2017, **46**, 2638–2648.

47 D. Balestri, P. P. Mazzeo, C. Carraro, N. Demitri, P. Pelagatti and A. Bacchi, *Angew. Chem., Int. Ed.*, 2019, **58**, 17342–17350.

48 D. Balestri, P. P. Mazzeo, R. Perrone, F. Fornari, F. Bianchi, M. Careri, A. Bacchi and P. Pelagatti, *Angew. Chem.*, 2021, **60**, 10194–10202.

49 L. R. Nassimbeni and H. Su, *CrystEngComm*, 2013, **15**, 7396–7401.

50 T. Le Roex, L. R. Nassimbeni and E. Weber, *Chem. Commun.*, 2007, 1124–1126.

51 http://www.who.int/medicines/publications/essentialmedicines/en/

52 T.-H. Wang, S.-M. Hsia, C.-H. Wu, S.-Y. Ko, M. Y. Chen, Y.-H. Shih, T.-M. Shieh, L.-C. Chuang and C.-Y. Wu, *PLoS One*, 2016, **11**, e0163147.

53 F. Diánez, M. Santos, C. Parra, M. J. Navarro, R. Blanco and F. J. Gea, *Lett. Appl. Microbiol.*, 2018, **67**, 400–410.

54 S. Borrego, O. Valdés, I. Vivar, P. Lavin, P. Guiamet, P. Battistoni, S. Gómez de Saravia and P. Borges, *ISRN Microbiol.*, 2012, **2012**, 1–7.

55 D. Balestri, A. Bacchi, P. Scilabra and P. Pelagatti, *Inorg. Chim. Acta*, 2018, **470**, 416–422.

56 K. Prout, J. Fail, R. M. Jones, R. E. Warner and J. C. Emmett, *J. Chem. Soc., Perkin Trans. 2*, 1988, 265–284.

57 A. Lausi, M. Polentarutti, S. Onesti, J. R. Plaisier, E. Busetto, G. Bais, L. Barba, A. Cassetta, G. Campi, D. Lamba, A. Pifferi, S. C. Mande, D. D. Sarma, S. M. Sharma and G. Paolucci, *Eur. Phys. J. Plus*, 2015, **130**, 43.

58 W. Kabsch, *Acta Crystallogr., Sect. D: Biol. Crystallogr.*, 2010, **66**, 125–132.

59 M. D. Winn, C. C. Ballard, K. D. Cowtan, E. J. Dodson, P. Emsley, P. R. Evans, R. M. Keegan, E. B. Krissinel, A. G. W. Leslie, A. McCoy, S. J. McNicholas, G. N. Murshudov, N. S. Pannu, E. A. Potterton, H. R. Powell, R. J. Read, A. Vagin, K. S. Wilson and IUCr, *Acta Crystallogr., Sect. D: Biol. Crystallogr.*, 2011, **67**, 235–242.

60 G. M. Sheldrick, *Acta Crystallogr., Sect. A: Found. Adv.*, 2015, **71**, 3–8.

61 O. V. Dolomanov, L. J. Bourhis, R. J. Gildea, J. A. K. Howard and H. Puschmann, *J. Appl. Crystallogr.*, 2009, **42**, 339–341.

62 G. M. Sheldrick, *Acta Crystallogr., Sect. C: Struct. Chem.*, 2015, **71**, 3–8.

63 A. Bacchi and P. P. Mazzeo, Cocrystallization as a tool to stabilize liquid active ingredients, *Crystallogr. Rev.*, 2021, DOI: 10.1080/0889311X.2021.1978079.

Footnotes

[†] Electronic supplementary information (ESI) available: Crystallography information, experimental details, host–guest and guest–guest contact analyses and guest occupancy details. CCDC 2094688–

2094690. For ESI and crystallographic data in CIF or other electronic format see DOI: 10.1039/d1ce00899d

Queries and Answers

Q1

Query: Have all of the author names been spelled and formatted correctly? Names will be indexed and cited as shown on the proof, so these must be correct. No late corrections can be made.

Answer: All names are correct

Q2

Query: Funder details have been incorporated in the funder table using information provided in the article text. Please check that the funder information in the table is correct.

Answer: Information are correct

Q3

Query: Please check that the inserted CCDC numbers are correct.

Answer: CCDC numbers are correct

Q4

Query: Please check that the ORCID iD provided for "Davide Balestri" is valid.

Answer: ORCID iD is valid for Davide Balestri

Q5

Query: The meaning of the phrase "returning the detailed mechanism governing the solvent-to-guest exchange positioning inside the channels featuring the framework of PUM168 were observed" in the sentence beginning "The adaptive behavior..." is not clear. Please provide alternative text.

Answer: done

Q6

Query: The caption to Fig. 1 has been altered for clarity. Please check that the meaning is correct.

Answer: Fig.1 caption is OK

Q7

Query: The sentence beginning "To extend the…" has been altered for clarity. Please check that the meaning is correct.

Answer: OK

Q8

Query: The sentence beginning “Propofol has two...” has been altered for clarity. Please check that the meaning is correct.

Answer: OK

Q9

Query: The sentence beginning “It is not...” has been altered for clarity. Please check that the meaning is correct.

Answer:

OK

Q10

Query: In the sentence beginning “Taking into account...” should “loading process efficient parameter” be changed to “loading efficiency parameter”?

Answer: OK

Q11

Query: The sentence beginning “For the sake...” has been altered for clarity. Please check that the meaning is correct.

Answer: OK

Q12

Query: The sentence beginning “The number of...” has been altered for clarity. Please check that the meaning is correct.

Answer: OK

Q13

Query: The sentence beginning “Also, the calculated...” has been altered for clarity. Please check that the meaning is correct.

Answer: OK

Q14

Query: The meaning of the phrase “looking at the different organization adopted by the same” in the sentence beginning “The adaptive behaviour...” is not clear. Please provide alternative text.

Answer: done

Q15

Query: The sentence beginning “The inclusion of...” has been altered for clarity. Please check that the meaning is correct.

Answer: OK

Q16

Query: The sentence beginning “Contrary to what...” has been altered for clarity. Please check that the meaning is correct.

Answer: OK

Q17

Query: The meaning of the phrase “guest imposed intermolecular contacts involving the amide groups” in the sentence beginning “The guest imposed...” is not clear. Please provide alternative text.

Answer: done

Q18

Query: In the sentence beginning “This adaptive behaviour...” should “at the base of” be changed to “the basis of”?

Answer: yes please.

Q19

Query: Have all of the funders of your work been fully and accurately acknowledged?

Answer: Yes, this paragraph is OK.